e-PROCEEDINGS

of The 5th International Conference on Computing, Mathematics and Statistics (iCMS2021)

4-5 August 2021

Driving Research Towards Excellence

e-Proceedings of the 5th International Conference on Computing, Mathematics and Statistics (iCMS 2021)

Driving Research Towards Excellence

e-ISBN: 978-967-2948-12-4
DOI

Library of Congress Control Number:

Publication by
Department of Mathematical Sciences
Faculty of Computer & Mathematical Sciences
UiTM Kedah

TABLE OF CONTENT

PART 1: MATHEMATICS

PART 2: STATISTICS

PART 3: COMPUTER SCIENCE & INFORMATION TECHNOLOGY

PART 4: OTHERS

UNSTEADY MHD CASSON FLUID FLOW IN A VERTICAL CYLINDER WITH POROSITY AND SLIP VELOCITY EFFECTS

Wan Faezah Wan Azmi[1], Ahmad Qushairi Mohamad[2], Lim Yeou Jiann[3], and Sharidan Shafie[4]
[1,2,3,4] Department of Mathematical Sciences, Faculty of Science, Universiti Teknologi Malaysia
([1] wanfaezah@graduate.utm.my, [2] ahmadqushairi@utm.my, [3] jiann@utm.my, [4] sharidan@utm.my)

The significance of Casson fluid flow in the cylinder has recently attracted many researchers to study analytically, numerically and experimentally due to its unique behavior and relation with the real-life applications such as blood flow in vessel tubes. Due to the lack of consideration for slip boundary conditions, this paper investigated analytically the effects of slip velocity and magnetic on the pulsatile flow of Casson fluid past through a vertical cylinder in a porous medium. The Casson fluid model was used under the influences of a uniformly distributed magnetic field, oscillating pressure gradient and porous medium in order to obtain governing equations. The analytical solutions of velocities were then solved by Laplace and finite Hankel transforms. These fluid velocities were then presented graphically. The result shows the slip velocity influenced the behavior of the Casson parameter and fluid velocity. Besides that, fluid velocity increases with the increase of Darcy number, while it decreases when the magnetic parameter increases. Thus, these findings are beneficial to explore further in the applications of biomedical engineering and pathology.

***Keywords*:** Casson fluid, MHD, porous medium, slip velocity, cylinder

1. Introduction

The study of viscous complex fluid is also known as non-Newtonian fluid attracted many researchers since it is widely used in science, industry and technology applications. The non-Newtonian fluid does not obey Newton's Law of viscosity which means it has a non-linear relationship or consists of yield stress between shear stress and shear rate (Alderman and Pipelines, 1977). One of the most popular and commonly used models is the Casson fluid model due to its applications in the field of metallurgy, food processing and bioengineering operations. Casson fluid is a shear thinning liquid with yield stress. It behaves like an elastic solid or liquid which depends on applied shear stress. Examples of Casson fluid are honey, paint, tomato sauce, jelly, blood due to its content such as plasma and protein and others (Chhabra, 2010). Many researchers study the Casson fluid flow in the cylindrical domain since it is more applicable to real-life applications such as flow in pipelines, flow in the blood vessel and others. An example of an early study was done by Shul'man (1973) which is studied Casson fluid flow past through cylinder and solved it numerically.

Magnetohydrodynamics (MHD) can be defined as the study concerned with exploring the effects of crossing magnetic fields within a moving electrically conducting fluid. MHD effects can be observed in many natural phenomena and industrial processes (Hamarsheh et al., 2020). Researchers are interested to study the MHD flow of Casson fluids since it plays a vital role to overcome blood disease problems and control blood flow in the artery. The earliest study has been done by Elshehawey et al. (2001) who investigated MHD effects on the blood flow. Later, Ali et al. (2017, 2018a, 2018b, 2019) solved problems for Casson fluid model as a blood model to analyze the effects of MHD flow in the cylinder with fixed and oscillated boundary conditions and MHD flow in the stenosed artery. They obtained analytical solutions for Casson fluid model by using Laplace and finite Hankel transform.

The study of fluid flow in porous medium provides another important characteristic to analyze the flow phenomenon. Examples in medical science applications are blood flow in an artery under some pathological situations when fatty plaques and blood clots are formed in the artery (Dash et al., 1996). Study magnetic field with the porous medium is significant. In the earliest studies, Rathod and Tanveer (2009) were obtained analytical solutions of MHD blood flow in porous medium past through a rigid cylinder by considering blood as a couple stress fluid. Then, Jamil and Zafarullah (2019) investigated MHD effects with the porous medium in the cylindrical domain for second-grade fluid. Abro and Atangana (2020) analyzed the porosity effects of MHD pulsatile flow by considering the Newtonian fluid model. All of them solved problems analytically by using Laplace and finite Hankel transform method but none of them discussed the Casson fluid model. Maiti et al. (2020) modelled blood as Casson fluid flowing in the fixed cylinder with MHD and porosity effects and later Maiti et al. (2021) extended the problem with the additional of chemical reaction effects. They obtained analytical solutions by using the same method as previous studies.

The slip velocity is defined as the finite velocity of a fluid at a boundary or surrounded within in that area (Nubar, 1971). The study of slip velocity at the boundary is significant on fluid velocity because it is influenced the viscosity and behavior of the fluid model. The earliest study of the effects of slip boundary conditions on the fluid flow in a channel was done by Rao and Rajagopal (1999). Then, Ahmed and Hazarika (2012) solved numerically the problem of Casson fluid flow as a blood model with MHD effect in slip velocity boundary at the cylinder. Ramesh and Devakar (2015) investigated some analytical solutions for Casson fluid flows in channel with slip boundary conditions. None of them used transformations of Laplace and Hankel to obtain analytical solutions. Laplace and Hankel transform methods are among the popular tools to solve the problem analytically. Jiang et al. (2017) and Shah et al. (2019) solved Oldroyd-B fluid flow in the cylindrical domain with the Navier slip velocity as a boundary condition. Then, Padma et al. (2019a, 2019b) discussed the effects of slip velocity and without slip velocity for the Jeffrey fluid flow in the cylinder with the presence of MHD.

To the best of the authors' knowledge, the analytical solution of the MHD Casson fluid flow model with the slip boundary conditions in a porous medium has not been presented in the existing literature. Therefore, the present work aims to investigate the unsteady pulsatile flow of Casson fluid past through a cylinder in a porous medium with MHD and slip velocity effects. The MHD Casson fluid flow was accelerated by the pressure gradient. Analytical solutions were calculated by Laplace and finite Hankel transforms. For the numerical analysis, zeros of the Bessel functions were used to obtain the graphical solutions by using Maple for different important parameters.

2. Mathematical Formulation

Consider the unsteady pulsatile flow of an incompressible Casson fluid in a vertical cylinder of radius, r_0. The z-axis is considered along the axis of the cylinder in a vertically upward direction and the r-axis be the radial direction. The schematic diagram explaining the problem is shown in Figure 1.

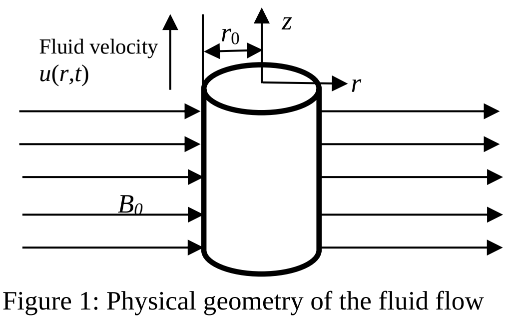

Figure 1: Physical geometry of the fluid flow

The fluid was driven by an oscillating pressure gradient and its flow was influenced by the external magnetic field and porous medium. It is assumed that the induced magnetic field, the external electric field and the electric field due to the polarization of charges are negligible. Initially, at time $t^*=0$, the fluid and cylinder are both at rest. Then, at the time $t^*>0$, the fluid begins to flow due to the slip velocity, u_s is applied at the boundary of the cylinder and the fluid has uniform flow velocity on the axis. Assume that the velocity is the function of r and t only. Then, the governing equation of Casson fluid flow in cylindrical polar coordinates by Maiti et al. (2020) can be written in the form of

$$\rho\frac{\partial u^*}{\partial t^*}=-\frac{\partial p^*}{\partial z^*}+\mu\left(1+\frac{1}{\beta}\right)\left(\frac{\partial^2 u^*}{\partial r^{*2}}+\frac{1}{r^*}\frac{\partial u^*}{\partial r^*}\right)-\frac{\mu}{k_p}u^*-\sigma B_0^2 u^* \tag{1}$$

with the associated initial and boundary conditions as

$$\begin{aligned} &u^*(r^*,0)=0 &&;\ r\in[0,r_0]\ , \\ &\frac{\partial u^*(0,t^*)}{\partial r^*}=0 &&;\ t^*>0, \\ &u^*(r_0^*,t^*)=u_s{}^* &&;\ t^*>0. \end{aligned} \tag{2}$$

Introducing the following dimensionless variables by Ali et al.(2018b), Mirza et al. (2019) and Padma et al. (2019a) as

$$t=\frac{t^*\nu}{r_0^2},\ \ r=\frac{r^*}{r_0},\ \ u=\frac{u^*}{u_0},\ \ u_s=\frac{u_s^*}{u_0},\ \ z^*=\frac{z}{r_0},\ \ p^*=\frac{pr_0}{\mu u_0} \tag{3}$$

where ρ is the density of the fluid, u^* is the velocity component along the z-axis, p is pressure gradient, μ is the dynamic viscosity of the fluid, β is the non-Newtonian Casson parameter, k_p is permeability constant, σ is electrical conductivity, B_0 is applied magnetic field strength and ν is the kinematic viscosity of the fluid. After employing the variables (3) into (1) and (2), it can be written in dimensionless form as

$$\frac{\partial u}{\partial t}=-\frac{\partial p}{\partial z}+\beta_1\left(\frac{\partial^2 u}{\partial r^2}+\frac{1}{r}\frac{\partial u}{\partial r}\right)-\frac{1}{Da}u-Mu \tag{4}$$

with the associated dimensionless initial and boundary conditions

$$\begin{aligned} &u(r,0)=0, &&;\ r\in[0,1]\ , \\ &\frac{\partial u(0,t)}{\partial r}=0, &&;\ t>0, \\ &u(1,t)=u_s, &&;\ t>0 \end{aligned} \tag{5}$$

where $Da=\dfrac{k_p}{r_0^2}$ is the Darcy number, $M=\dfrac{\sigma B_0^2 r_0^2}{\rho\nu}$ is the magnetic parameter, $\beta_1=\dfrac{1}{\beta_0}$ and $\beta_0=1+\dfrac{1}{\beta}$ are the constant parameters. The periodic pressure gradient emerging from pumping action of the heart can be put mathematically as (Maiti et al., 2020)

$$-\frac{\partial p}{\partial z}=A_0+A_1\cos\left(\omega t\right) \tag{6}$$

where A_0 and A_1 are the constants and pulsatile amplitude, ω defines as pulsatile frequency. Rewrite (4) with subject to (6), yields

$$\frac{\partial u}{\partial t}=\left(A_0+A_1\cos\left(\omega t\right)\right)+\beta_1\left(\frac{\partial^2 u}{\partial r^2}+\frac{1}{r}\frac{\partial u}{\partial r}\right)-\frac{1}{Da}u-Mu. \tag{7}$$

3. Problem Solution

The joint Laplace transform and finite Hankel transform have been used to find analytical solutions of (7). By applying Laplace transform into (7) subjected to the initial condition (5), yields

$$s\bar{u}(r,s)=\frac{A_0}{s}+\frac{A_1 s}{s^2+\omega^2}+\beta_1\left[\frac{\partial^2\bar{u}(r,s)}{\partial r^2}+\frac{1}{r}\frac{\partial\bar{u}(r,s)}{\partial r}\right]-\frac{1}{Da}\bar{u}(r,s)-M\bar{u}(r,s) \tag{8}$$

with boundary conditions

$$\frac{\partial\bar{u}(0,s)}{\partial r}=0, \qquad \bar{u}(1,s)=\frac{u_s}{s} \tag{9}$$

where $\bar{u}(r,s)$ is the Laplace transform of the function $u(r,t)$ and s is the transform variable. Then, apply finite Hankel transform of zero-order to (8) and by using condition (9), gives

$$\bar{u}_H(r_n,s)=\left[\left(\frac{A_0}{s}+\frac{A_1 s}{s^2+\omega^2}\right)\frac{J_1(r_n)}{r_n}+\frac{\beta_1 r_n J_1(r_n)u_s}{s}\right]\frac{1}{s+F_3} \tag{10}$$

where $F_3=\dfrac{1+Da\left(M+\beta_1 r_n^2\right)}{Da}$ and $\bar{u}_H(r_n,s)=\int_0^1 r\bar{u}(r,s)J_0(rr_n)\,dr$ is the finite Hankel transform of the function $\bar{u}(r,s)$ and r_n with $n=0,1,\ldots$ are the positive roots of the equation $J_0(x)=0$, where J_0 is being the Bessel function of the first kind and zero order. Rearrange (10) as follows:

$$\bar{u}_H(r_n,s)=\left(\bar{F}_4(s)+\bar{F}_5(s)\right)\frac{J_1(r_n)}{r_n}+\beta_1 r_n J_1(r_n)\bar{F}_6(s) \tag{11}$$

where $F_4(s)=\dfrac{A_0}{F_3}\left(\dfrac{1}{s}-\dfrac{1}{s+F_3}\right)$, $F_5(s)=\dfrac{A_1 s}{s^2+\omega^2}\dfrac{1}{s+F_3}$ and $F_6(s)=\dfrac{u_s}{F_3}\left(\dfrac{1}{s}-\dfrac{1}{s+F_3}\right)$.

Applying the inverse Laplace transform to (11), give

$$u_H(r_n,t)=\left(f_4(t)+f_5(t)\right)\frac{J_1(r_n)}{r_n}+\beta_1 r_n J_1(r_n)f_6(t) \tag{12}$$

where $f_4(t)=\dfrac{A_0}{F_3}\left(1-\exp(-F_3 t)\right)$, $f_5(t)=\dfrac{A_1}{F_3^2+\omega^2}\left(F_3\cos(\omega t)+\omega\sin(\omega t)-F_3\exp(-F_3 t)\right)$ and $f_6(t)=\dfrac{u_s}{F_3}\left(1-\exp(-F_3 t)\right)$.

Finally, the analytical solution of fluid velocity is obtained by taking the inverse finite Hankel transform of zero-order to (12). Subsequently, this equation can be simplified as follows:

$$u(r,t)=2\sum_{n=1}^{\infty}u_H(r_n,t)\frac{J_0(rr_n)}{J_1^2(r_n)}, \tag{13}$$

$$\begin{aligned} u(r,t)=u_s-2u_s\sum_{n=1}^{\infty}&\left[\exp(-F_3t)+\frac{c(1-\exp(-F_3t))}{c+\beta_1 r_n^2}\right]\frac{J_0(rr_n)}{r_nJ_1(r_n)} \\ &+2\sum_{n=1}^{\infty}\left[\frac{A_0}{F_3}(1-\exp(-F_3t))\right]\frac{J_0(rr_n)}{r_nJ_1(r_n)} \\ &+2\sum_{n=1}^{\infty}\left[\frac{A_1}{F_3^2+\omega^2}\left(F_3(\cos(\omega t)-\exp(-F_3t))+\omega\sin(\omega t)\right)\right]\frac{J_0(rr_n)}{r_nJ_1(r_n)} \end{aligned} \tag{14}$$

where $c=\frac{1}{Da}+M$ is constant parameter.

4. Result and Discussion

The impact of different fluid parameters on fluid velocity $u(r,t)$ has been discussed graphically by using the MAPLE as a computational tool in Figures 2-7. These parameters include Casson parameter β, magnetic parameter M, Darcy number Da, slip velocity parameter u_s and time parameter t. The following parameters are fixed for the numerical computations: A_0=0.05, A_1=0.05, $\omega=\pi/4$, β=1.2, Da=1.0, M=1.0, t=1.0, u_s=0.1 and range values of related parameters have been estimated as: β=0.4,0.8,1.2, M=0,1.0,2.0, Da=1.0,2.0,3.0 (Padma et al., 2019; Maiti et al., 2021). However, to describe the results of the current study, wide spectrum values of parameters had been used as t=0.2,5.0,10 and u_s=0,0.01,0.06,0.1.

Figure 2 illustrates the velocity profiles for different values of Casson parameter, β with the presence of slip velocity and no-slip velocity effects. It is shown that slip velocity influences the behavior of the Casson parameter and fluid velocity. The velocity profiles decrease with an increase in the Casson parameter, whilst the velocity increases as the slip velocity increase. Generally, increases in the Casson parameters will cause decreases in the yield stress and increases in the plastic dynamic viscosity. Consequently, it creates resistance in the flow of fluid. However, the existence of a larger slip velocity at the wall of the cylinder influences the viscosity and plasticity behavior of Casson. Figure 3 depicts the velocity profiles for different values of Casson parameter, β and time, t with a fixed value of slip velocity. It is found that fluid velocity increases as β and t increase for a large value of slip velocity.

Figures 4 and 5 present the velocity profiles for different values of magnetic parameter M. It is observed that fluid velocity decreases as the magnetic parameter increases. It is due to electric current is generated when the external magnetic field is applied to moving electrically conducting fluid. Interaction between induced currents and magnetic field produces a resistive force known as Lorentz force, which acts in the opposite direction of the fluid motion and tends to resist the flow. In addition, fluid velocity decreases towards the center of the cylinder as a larger slip velocity has occurred. Meanwhile, fluid velocity increases as t increases. It is due to the fluid system is achieved the flow stability for a larger time parameter.

Figures 6 and 7 display velocity profiles for different values of the Darcy number, Da. It is found that fluid velocity increases as Da increases due to increases permeability of the porous medium. Increase in permeability means increase in the ability of the porous medium to allow fluid to pass through it. As an outcome, velocity inclines for slip and no-slip boundary conditions. Besides that, the presence of larger slip velocity results in decreasing of fluid velocity as it is approaching towards the center of the cylinder. It is due to the boundary layer thickness of Casson fluid increasing towards the center. Thus, fluid velocity increases as Da and t increase.

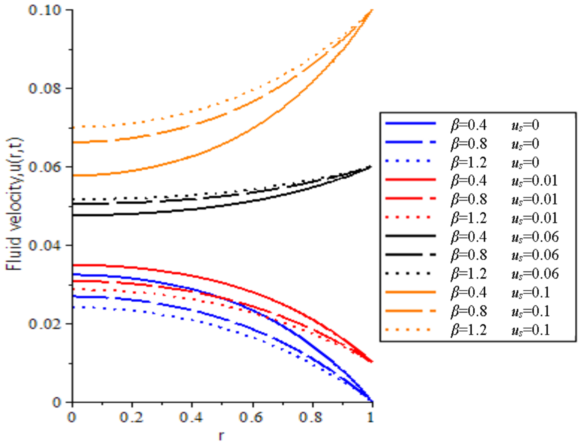

Figure 2: Velocity profiles $u(r,t)$ at different values of Casson parameter, β and slip velocity, u_s

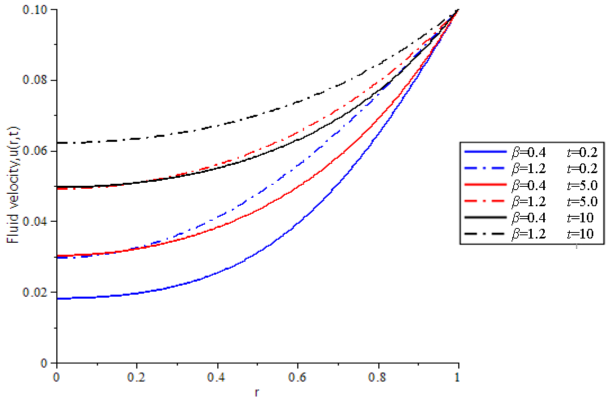

Figure 3: Velocity profiles $u(r,t)$ at different values of Casson parameter, β and time, t

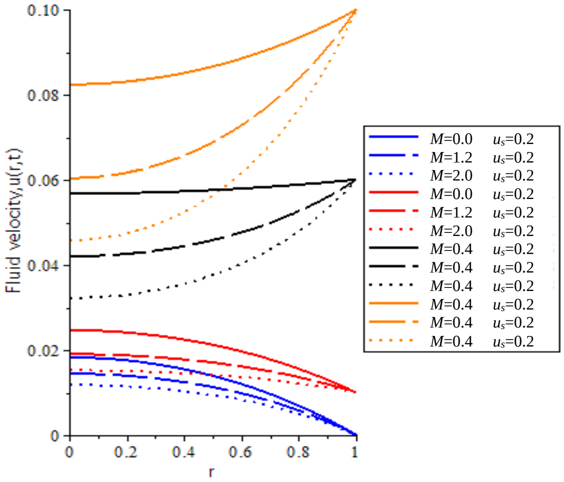

Figure 4: Velocity profiles $u(r,t)$ at different values of magnetic parameter, M and slip velocity, u_s

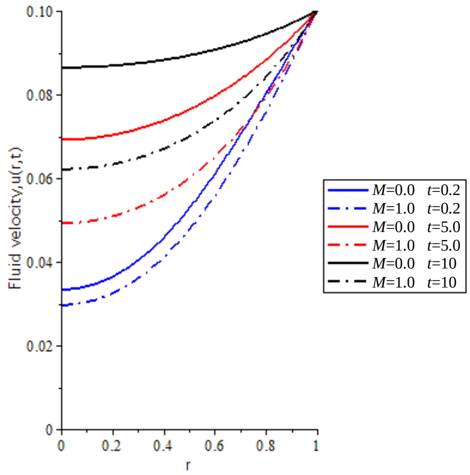

Figure 5: Velocity profiles $u(r,t)$ at different values of magnetic parameter, M and time, t

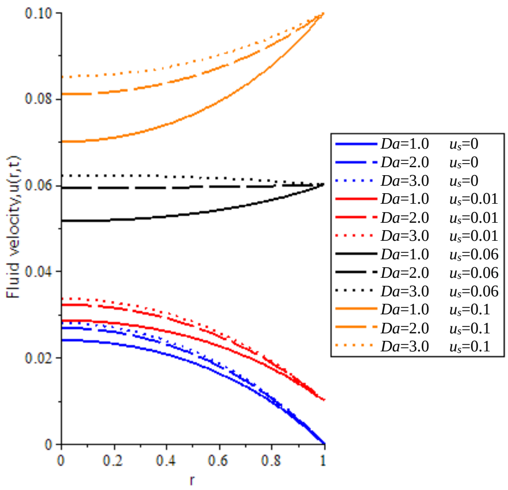

Figure 6: Velocity profiles $u(r,t)$ at different values of Darcy number, Da and slip velocity, u_s

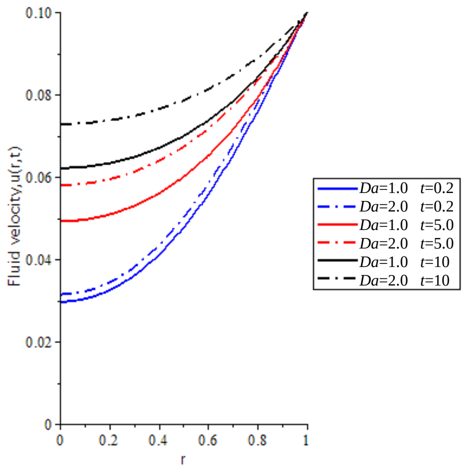

Figure 7: Velocity profiles $u(r,t)$ at different values of Darcy number, Da and time, t

5. Conclusion

This paper presents the analysis of Casson fluid flow in the vertical cylinder with slip boundary conditions subjected to the magnetic field and porosity effects. The analytical solution of the governing equation has been obtained by using the Laplace and finite Hankel transforms of order zero. The viscosity and plasticity of Casson fluid are influenced by the slip velocity at the boundary conditions. For larger slip velocity, increases of β results in increases in fluid velocity while for no-slip velocity or small slip velocity, increases of β will cause decreases in fluid velocity. Besides that, fluid velocity increases with increases of Da and t. Meanwhile, fluid velocity decreases as the magnetic parameter increases. These findings are beneficial for studying real-life applications in biomedical engineering and pathology.

Acknowledgment

The authors would like to acknowledge the Ministry of Higher Education Malaysia and Research Management Centre-UTM, University Technology Malaysia (UTM) for financial support through vote numbers [17J98, FRGS/1/2019/STG06/UTM/02/22 and 08G33].

References

Abro, K. A. and Atangana, A. (2020). Porous effects on the fractional modeling of magnetohydrodynamic pulsatile flow: an analytic study via strong kernels. *Journal of Thermal Analysis and Calorimetry*. https://doi.org/10.1007/s10973-020-10027-z

Ahmed, S. and Hazarika, G. C. (2012). Casson fluid Model for Blood flow with Velocity Slip in presence of Magnetic effect. *International Journal of Sciences: Basic and Applied Research*, 5(1):1–8.

Alderman, N. J. and Pipelines, S. (1977). Non-Newtonian Fluids: Guide to Classification and Characteristics. https://www.researchgate.net/publication/273392367_Non- Newtonian_Fluids_ Guide_to_Classification_and_Characteristics

Ali, F., Sheikh, N.A., Khan, I., and Saqib, M. (2017). Magnetic field effect on blood flow of Casson fluid in axisymmetric cylindrical tube: A fractional model. *Journal of Magnetism and Magnetic Materials*, 423(September 2016): 327–336.

Ali, F., Imtiaz, A., Khan, I., and Sheikh, N.A. (2018a). Flow of magnetic particles in blood with isothermal heating: A fractional model for two-phase flow. *Journal of Magnetism and Magnetic Materials*, 456:413–422.

Ali, F., Imtiaz, A., Khan, I., and Sheikh, N.A. (2018b). Hemodynamic flow in a vertical cylinder with heat transfer: Two-phase caputo fabrizio fractional model. *Journal of Magnetics*, 23(2):179–191.

Ali, F., Khan, N., Imtiaz, A., Khan, I., and Sheikh, N.A. (2019). The impact of magnetohydrodynamics and heat transfer on the unsteady flow of Casson fluid in an oscillating cylinder via integral transform: A Caputo–Fabrizio fractional model. *Pramana - Journal of Physics*, 93(3):1–12.

Chhabra, R. P. (2010). Non-Newtonian Fluids : An Introduction. *SERC School-cum-Symposium on Rheology of complex fluids*, 1–33.

Dash, R. K., Mehta, K. N. and Jayaraman, G. (1996). Casson fluid flow in a pipe filled with a homogeneous porous medium. *Int. J. Engng Sci.*, 34(10):1145–1156.

Elshehawey, E. F., Elbarbary, E.M.E., Afifi, N.A.S., and El-Shahed, M. (2001). MHD flow of blood under body acceleration. *Integral Transforms and Special Functions*, 12(1):1–6.

Hamarsheh, A. S., Alwawi, F. A., Alkasasbeh, H. T., Rashad, A. M., and Idris, R. (2020). Heat Transfer Improvement in MHD Natural Convection Flow of Graphite Oxide / Carbon Nanotubes-Methanol Based Casson Nanofluids past a Horizontal Circular Cylinder. *Processes*, 8(11):1444.

Jamil, M. and Zafarullah, M. (2019). MHD flows of second grade uid through the moving porous cylindrical domain. *European Journal of Pure and Applied Mathematics*, 12(3):1149–1175.

Jiang, Y., Qi, H., Xu, H., and Jiang, X. (2017). Transient electroosmotic slip flow of fractional Oldroyd-B fluids. *Microfluidics and Nanofluidics*. https://doi.org/10.1007/s10404-016-1843-x

Maiti, S., Shaw, S. and Shit, G. C. (2020). Caputo–Fabrizio fractional order model on MHD blood flow with heat and mass transfer through a porous vessel in the presence of thermal radiation. *Physica A: Statistical Mechanics and its Applications*, 540:123149.

Maiti, S., Shaw, S. and Shit, G. C. (2021). Fractional order model for thermochemical flow of blood with Dufour and Soret effects under magnetic and vibration environment. *Colloids and Surfaces B: Biointerfaces*, 197(October 2020):111395.

Mirza, I. A., Akram, M. S. and Siddique, I. (2019). Flows of a generalized second grade fluid in a cylinder due to a velocity shock. *Chinese Journal of Physics*, 60(November 2018): 720–730.

Nubar, Y. (1971). Blood Flow, Slip, and Viscometry. *Biophysical Journal*. https://doi.org/10.1016/S0006-3495(71)86212-4.

Padma, R., Ponalagusamy, R. and Tamil Selvi, R. (2019a). Mathematical modeling of electro hydrodynamic non-Newtonian fluid flow through tapered arterial stenosis with periodic body acceleration and applied magnetic field. *Applied Mathematics and Computation*. 362:124453.

Padma, R., Selvi, R. T. and Ponalagusamy, R. (2019b). Effects of slip and magnetic field on the pulsatile flow of a Jeffrey fluid with magnetic nanoparticles in a stenosed artery. *The European Physical Journal Plus*. https://doi.org/10.1140/epjp/i2019-12538-9.

Ramesh, K. and Devakar, M. (2015). Some analytical solutions for flows of Casson fluid with slip boundary conditions. *Ain Shams Engineering Journal*. 6(3):967–975.

Rao, I. J. and Rajagopal, K. R. (1999). Effect of the slip boundary condition on the flow of fluids in a channel. *Acta Mechanica*, 135(3):113–126.

Rathod, V. P. and Tanveer, S. (2009). Pulsatile flow of couple stress fluid through a porous medium with periodic body acceleration and magnetic field. *Bulletin of the Malaysian Mathematical Sciences Society*, 32(2):245–259.

Shah, N. A., Wang, X., Qi, H., Wang, S. and Hajizadeh, A. (2019). Transient electro-osmotic slip flow of an Oldroyd-B fluid with time-fractional Caputo-Fabrizio derivative. *Journal of Applied and Computational Mechanics*, 5(4):779–790.

Shul’man, Z. P. (1973). Calculation of a Laminar Axial Flow of a Nonlinear Viscoplastic medium in an annular channel. *Inzherno-Fizieheskii Zhurnal*, 19(4):1283–1289.

2021 ICMS

INTERNATIONAL CONFERENCE ON COMPUTING, MATHEMATICS AND STATISTICS

e ISBN 978-967-2948-12-4